Supporting Information

Ultrasmall Nickel Nanoparticles on a Covalent Triazine Framework for Ammonia Borane Hydrolysis and Transfer Hydrogenation of Nitroaromatics

Esther Punzi,[a] Xuan Trung Nguyen,[a] Emanuela Pitzalis,[a] Alessandro Mandoli,[b] Massimo Onor,[a] Marcello Marelli,[c] Lorenzo Poggini,[d,e] Giulia Tuci,[d] Giuliano Giambastiani,[d,e] Claudio Evangelisti[a]**

[a] Institute of Chemistry of Organo Metallic Compounds, CNR-ICCOM, Via G. Moruzzi 1, 56124 Pisa, Italy;

[b] Department of Chemistry and Industrial Chemistry, University of Pisa, Via G. Moruzzi 13, 56124 Pisa, Italy;

[c] Institute of Science and Chemical Technologies "Giulio Natta", CNR-SCITEC, Via Fantoli 16/15, 20138 Milano, Italy;

[d] Institute of Chemistry of Organo Metallic Compounds, CNR-ICCOM, Via Madonna del Piano 10, Sesto Fiorentino, Italy;

[e]Department of Chemistry "U. Schiff" - DICUS – and INSTM Research Unit, University of Florence, Via della Lastruccia 3-13, 50019 Sesto Fiorentino (FI), Italy.

Corresponding Authors: Giuliano Giambastiani (giuliano.giambastiani@iccom.cnr.it); Claudio Evangelisti (claudio.evangelisti@cnr.it)

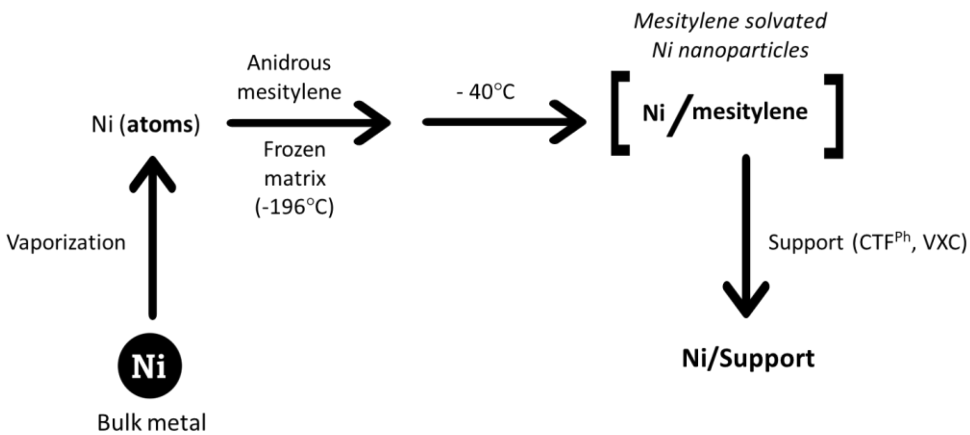

Figure S1. General procedure for the preparation of Ni catalyst by MVS approach

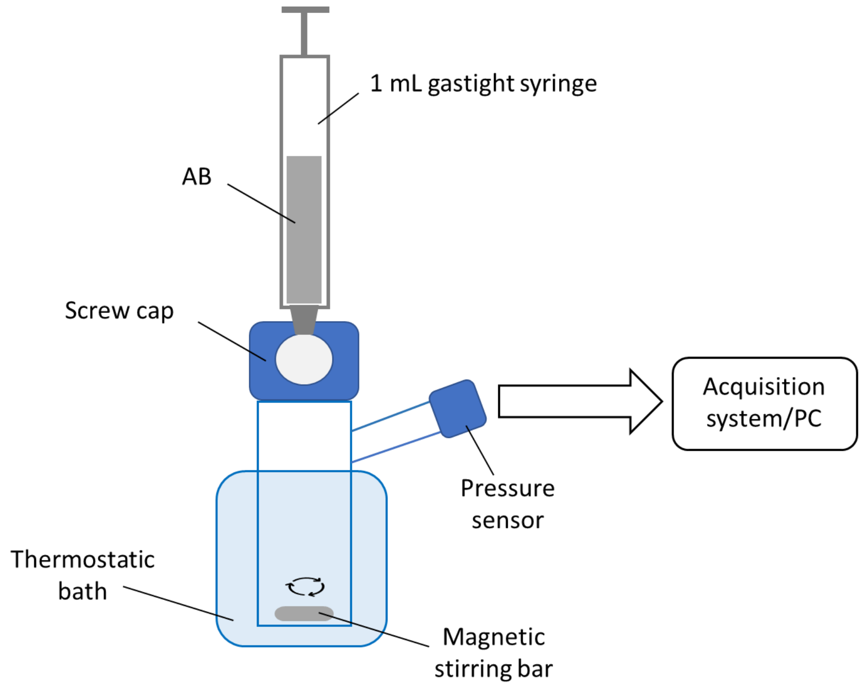

Figure S2. Schematic representation of the experimental setup employed for hydrogen evolution measures and hydrogenation reactions in batch conditions.

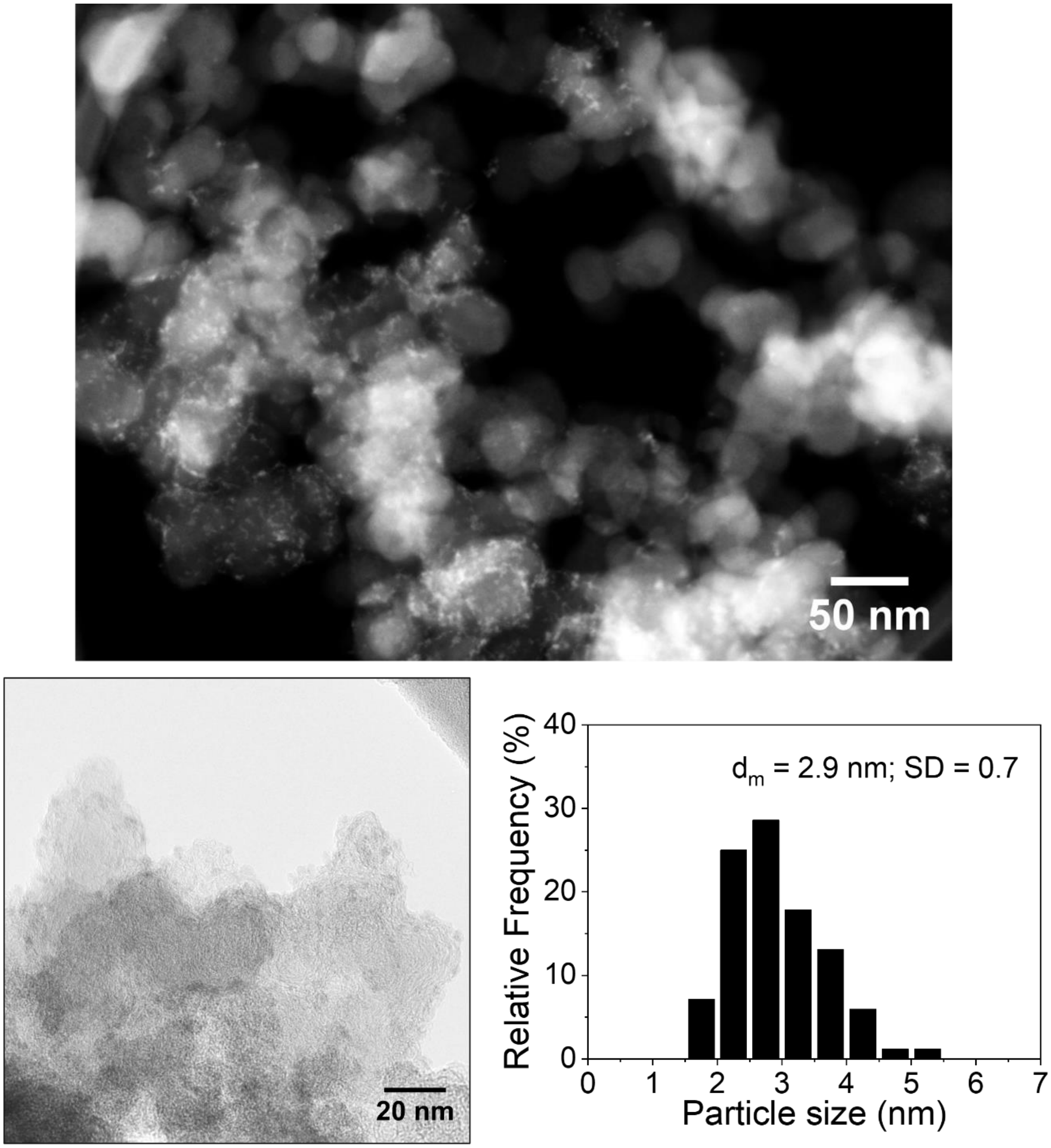

Figure S3. Representative HAADF-STEM micrograph (top), TEM micrograph (bottom left) and estimated particle size distribution (bottom right) of Ni/VXC (**2**).

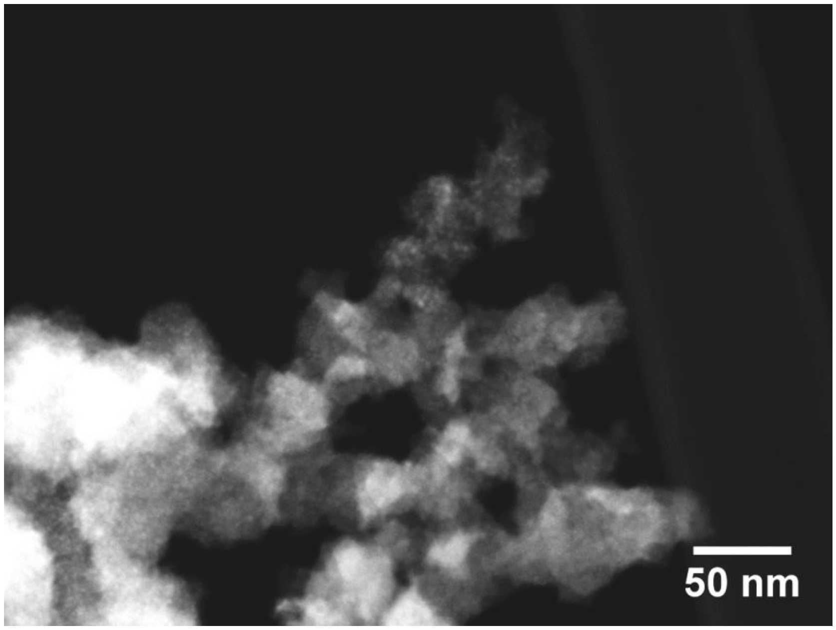

Figure S4. Representative HAADF-STEM micrograph of Ni/CTF^{Ph} (**1**).

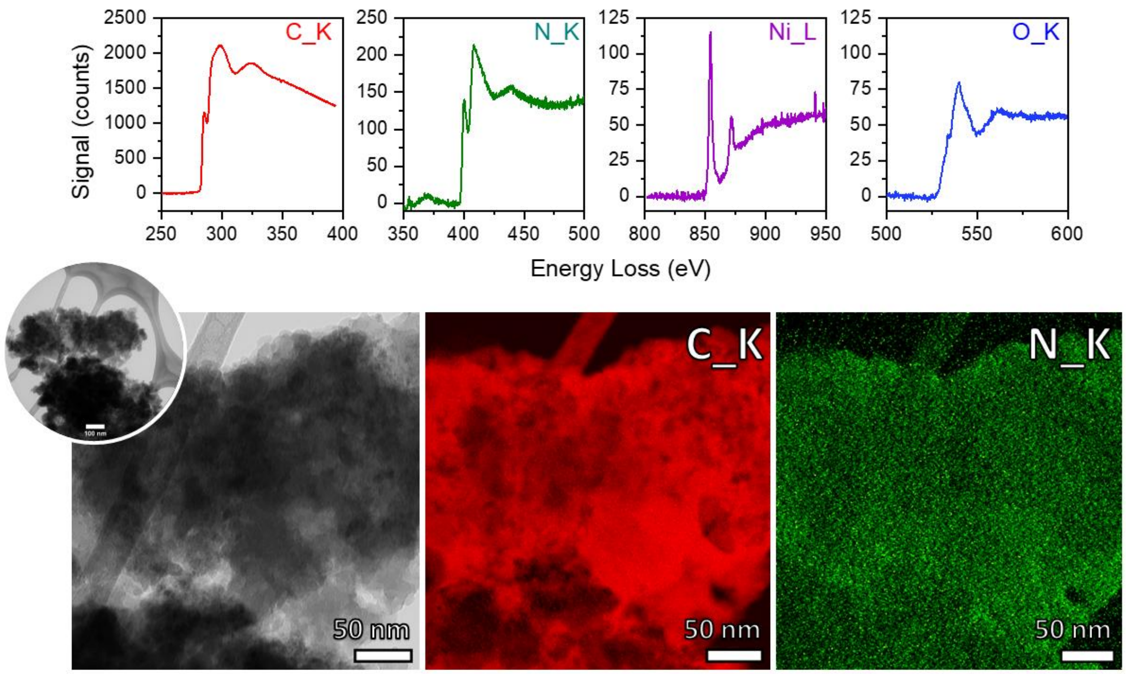

Figure S5. Above: Electron Energy-Loss Spectroscopy (EELS) spectra of Ni/CTF^{Ph} (**1**) collected at the K-Edge of Carbon, Nitrogen, and Oxygen, and at the $L_{2,3}$-Edge of Nickel. The shape and shift of Ni $L_{2,3}$-Edges at 854 eV and 873 eV suggest the presence of NiO species. Below: electron spectroscopic imaging (ESI) acquisition at a selected and representative sample area at K-Edges of Carbon and Nitrogen. N.b. in the N_K map, faded signals from the lacey carbon layer in the upper part of the image are an artifact generated by the drift correction applied during the image rielaboration.

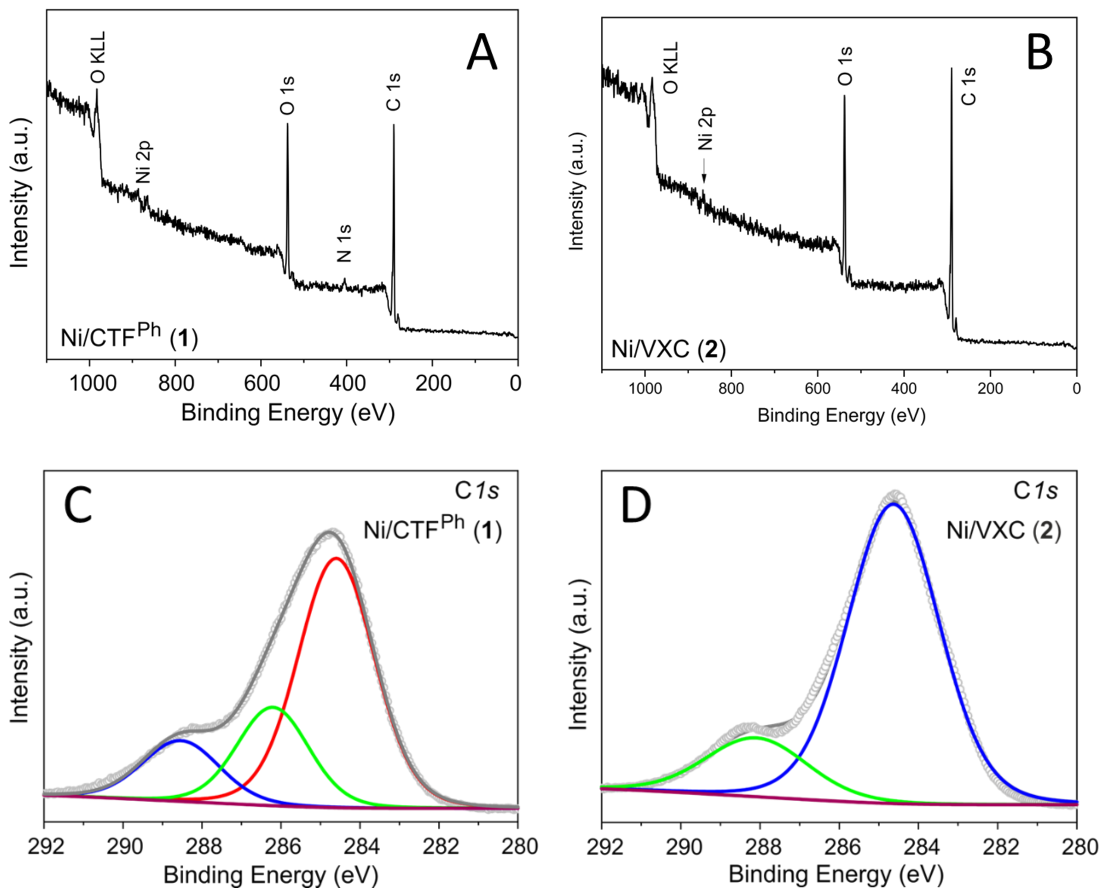

Figure S6. Survey spectra of both samples highlighted the expected elemental composition made of C, N, O and Ni and C, O and Ni for **1** (**A**) and **2** (**B**), respectively. High resolution C 1*s* spectra of **1** (**C**) and **2** (**D**), respectively.

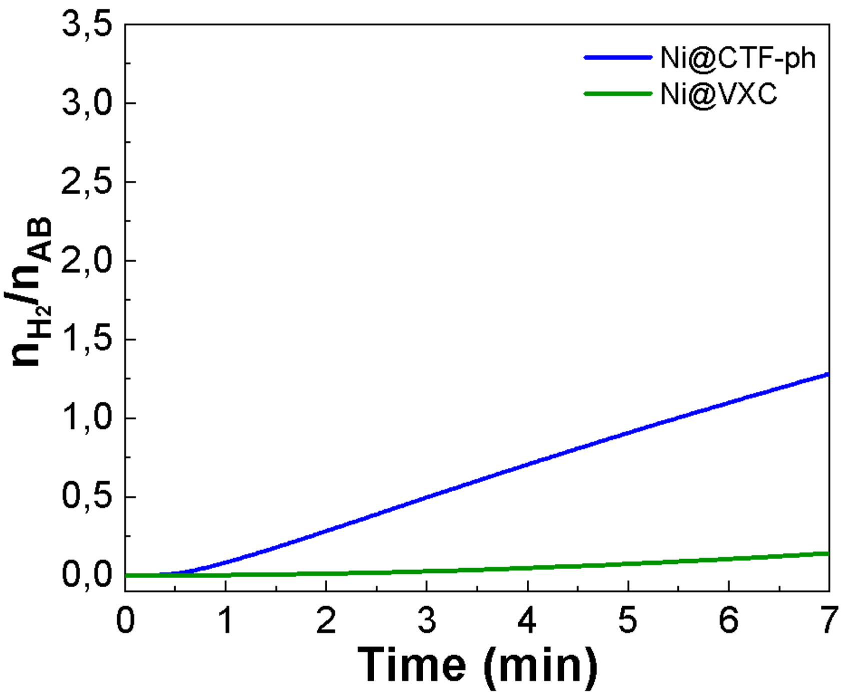

Figure S7. Magnification of the first 7 minutes of the AB hydrolysis catalyzed by Ni/CTF^{Ph} (**1**, green line), Ni/VXC (**2**, blue line), respectively, at 45°C.

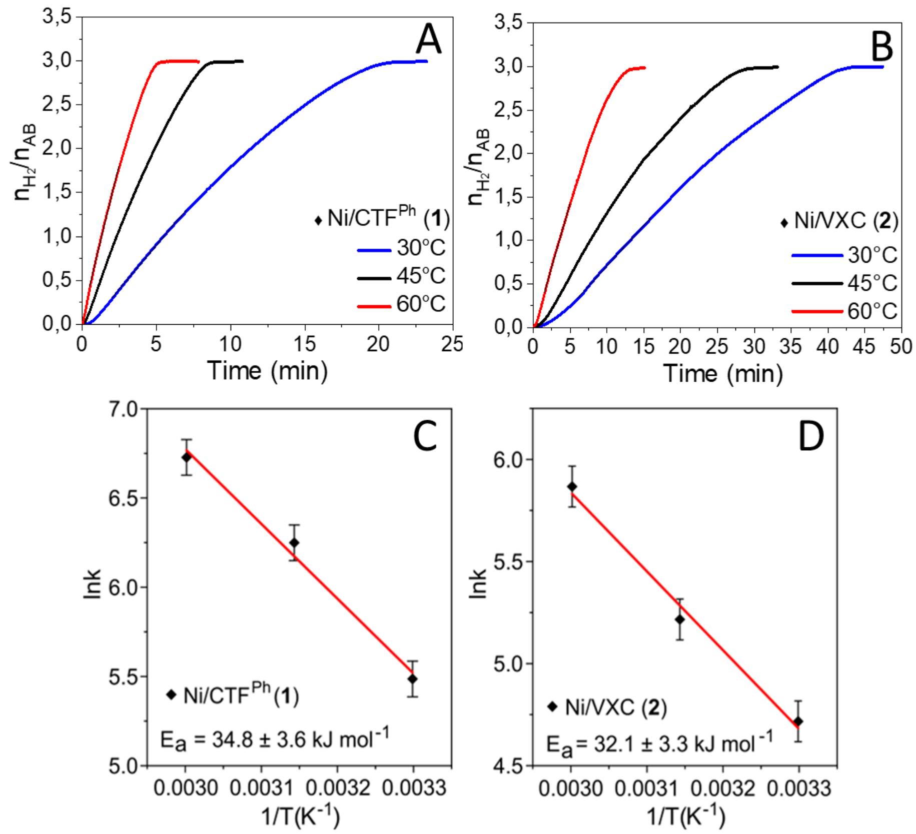

Figure S8. H_2 evolution in AB hydrolysis registered with Ni/CTF^{Ph} (**1**) (**A**) and Ni/VXC (**2**) (**B**) at different temperatures (30, 45, 60°C). Corresponding Arrhenius plots obtained from the kinetic data recorded for Ni/CTF^{Ph} (**1**) (**C**) and Ni/VXC (**2**) (**D**).

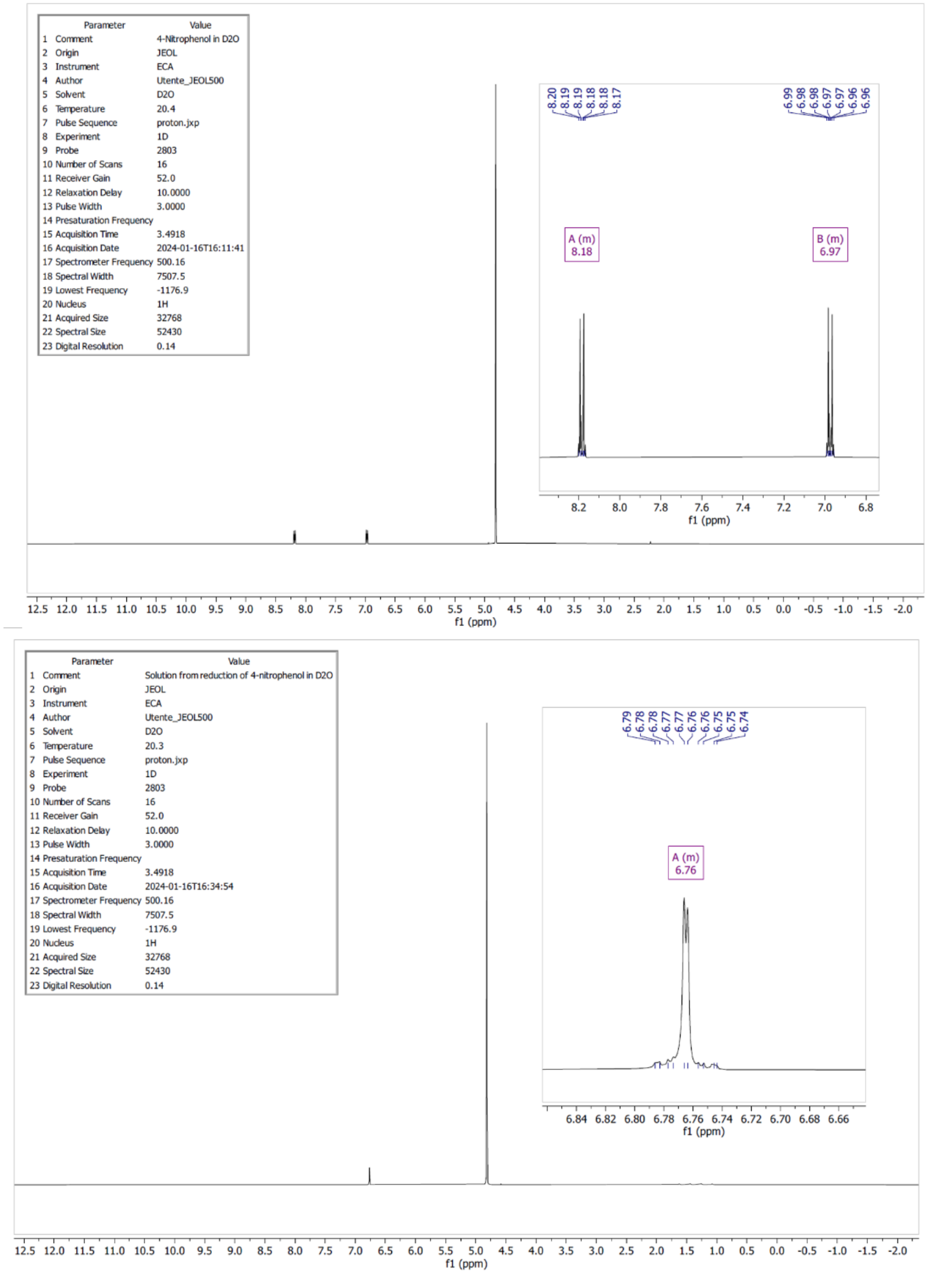

Figure S9. ^{1}H-NMR spectra of p-nitrophenol substrate (top) and the crude reaction mixture (bottom) relative to catalytic reaction performed in D_2O in the conditions reported in entry 1 of Table 2.

4-Nitrophenol (top)
^{1}H NMR (500 MHz, D_2O): 8.21 – 8.16 (m, 2H), 7.00 – 6.95 (m, 2H).
4-Aminophenol (bottom)
^{1}H NMR (500 MHz, D_2O): 6.79 – 6.74 (m, 4H).

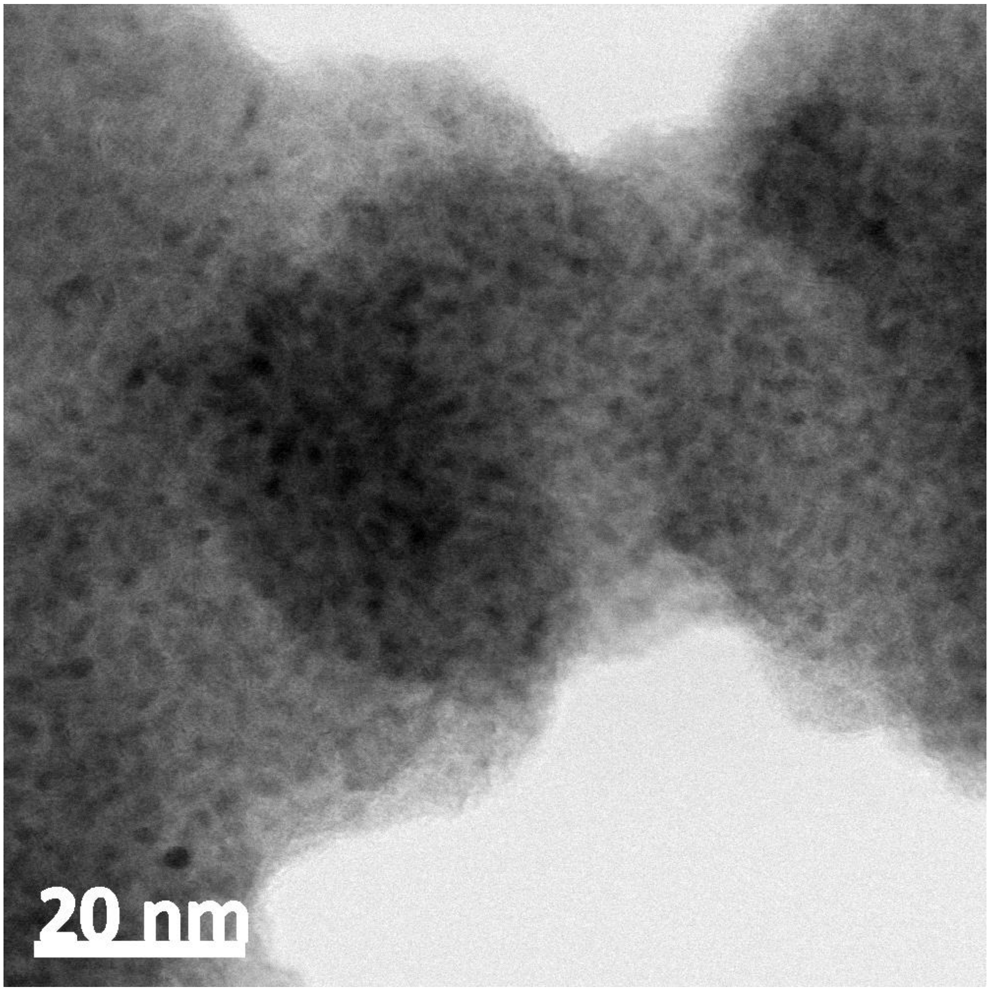

Figure S10. Representative micrograph of the Ni/CTF^{Ph} recovered after six reaction runs.

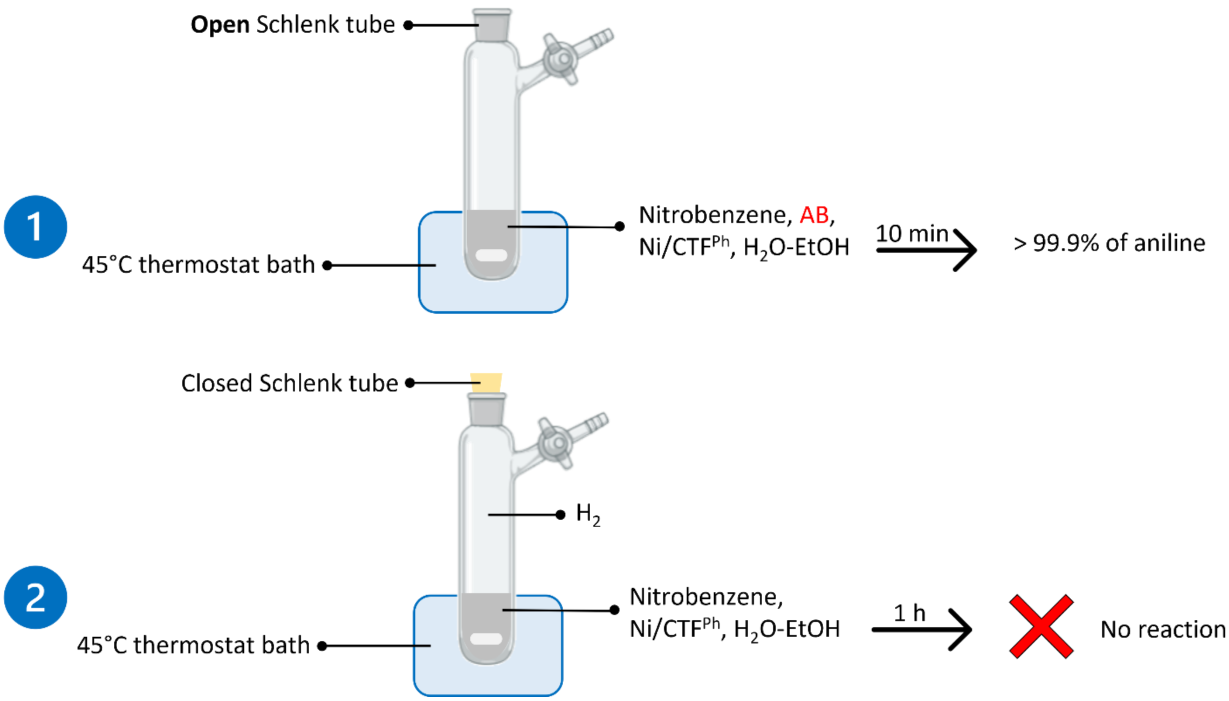

Figure S11. Graphical representation of the experimental tests carried out to investigate the reaction mechanism.

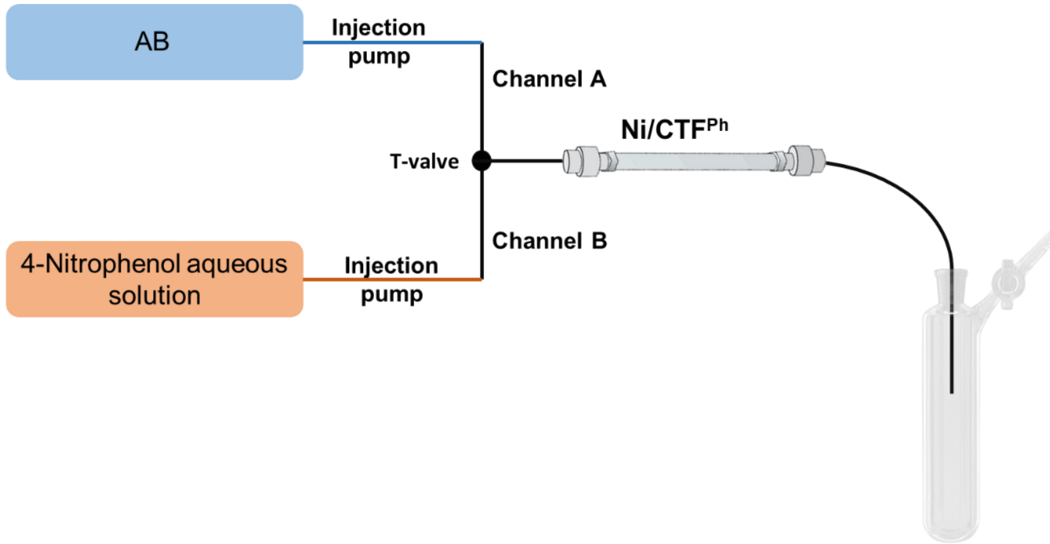

Figure S12. Schematic diagram of the continuous-flow reactor used for the catalytic AB TH to 4-nitrophenol.

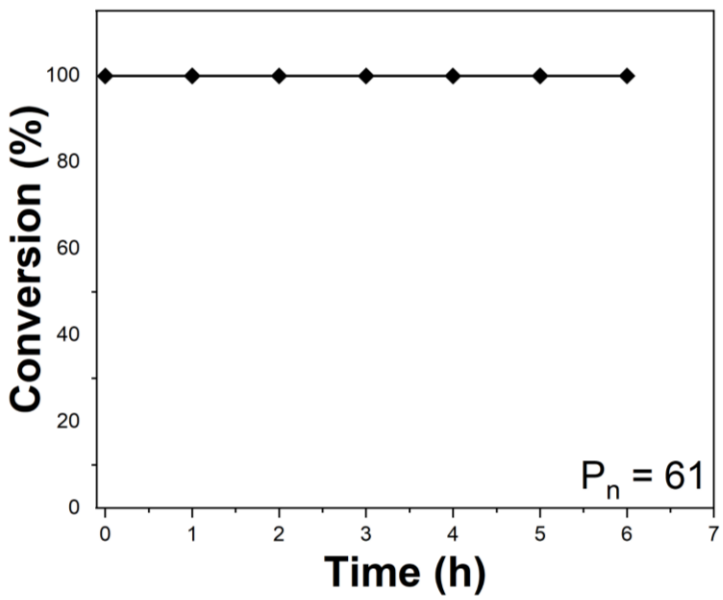

Figure S13. Continuous-flow AB TH to nitrophenol catalyzed by Ni/CTF^{Ph} (10.0 wt.%, 34.8 mg, 0.059 mmol Ni). Reaction conditions for each run : 0.5 M AB (4.2 mmol, f_A = 70 μL min^{-1}), 0.017 M 4-nitrophenol (0.83 mmol, f_B = 407 μL min^{-1}), T = 45 °C, t = 2 h.

Table S1. Comparative analysis of the Turnover Frequency (TOF) of various Ni catalysts of the *state-of-the-art* with Ni/CTF^{Ph} in the reaction of AB hydrolysis.

Entry	Catalyst	TOF [min^{-1}]	T [°C]	Reference
1	Ni/CTF^{Ph}	14.3	30	This study
2	CVD-Ni@ZIF-8	14.2	R.T.	[1]
3	Ni/SiO_2	13.2	25	[2]
4	3.2 nm Ni/C	8.8	25	[3]
5	5% Ni/CTF-1	8.7	25	[4]
6	CLD-Ni@ZIF-8	8.4	R.T.	[1]
7	Ni/KB	7.4	25	[5]
8	5% Ni/CNT	5.4	25	[4]
9	Hollow-Ni NPs	4.3	R.T.	[6]
10	Ni@h-BN	4.1	25	[7]
11	5% Ni/AC	2.6	25	[4]
12	Ni/BN sheets	1.2	25	[8]

Table S2. Summary of reaction conditions for the reduction of nitroarenes using different Ni catalysts and different hydrogen sources.

Entry	Catalyst	Hydrogen source	Temperature [°C]	Time [h]	n_{sub}/n_{Ni}	Reference
1	Ni@CTF^{ph}	AB	45	0.08 - 1.8	20	This study
2	Ni@N-CNTs-GS	H_2	110 - 120	1.7 - 6	11	[9]
3	Ni-N-C-700	H_2	130	10	84	[10]
4	Ni@NC-400	H_2	100	0.3 - 5.4	8	[11]
5	Ni@NC-1	H_2	100	1.5 - 2.5	4-8	[12]
6	Ni/r-SiO_2-CIS	H_2	150	4 - 12	22	[13]
7	Ni/CeO_2-CAS	H_2	210	6.5 - 8	25	[14]
8	H-Ni@NC-600	NH_2-NH_2	60	0.5 - 2	16	[15]
9	Ni SAs/NHCS	NH_2-NH_2	60	0.3 - 7	59	[16]
10	Ni-pol	$NaBH_4$	RT	5	54	[17]
11	Ni-HBP-3	HCOOH	RT	12	3.3	[18]
12	NiMCM-41	iPrOH	83	2.5 - 5.5	273	[19]

REFERENCES

(1) Li, P. Z.; Aranishi, K.; Xu, Q. ZIF-8 Immobilized Nickel Nanoparticles: Highly Effective Catalysts for Hydrogen Generation from Hydrolysis of Ammonia Borane. *Chem. Comm.* **2012**, *48* (26), 3173-3175.

(2) Metin, Ö.; Özkar, S.; Sun, S. Monodisperse Nickel Nanoparticles Supported on SiO2 as an Effective Catalyst for the Hydrolysis of Ammonia-Borane. *Nano. Res.* **2010**, *3* (9), 676–684.

(3) Metin, Ö.; Mazumder, V.; Özkar, S.; Sun, S. Monodisperse Nickel Nanoparticles and Their Catalysis in Hydrolytic Dehydrogenation of Ammonia Borane. *J. Am. Chem. Soc.* **2010**, *132* (5), 1468–1469.

(4) Li, Z.; He, T.; Liu, L.; Chen, W.; Zhang, M.; Wu, G.; Chen, P. Covalent Triazine Framework Supported Non-Noble Metal Nanoparticles with Superior Activity for Catalytic Hydrolysis of Ammonia Borane: From Mechanistic Study to Catalyst Design. *Chem. Sci.* **2016**, *8* (1), 781–788.

(5) Guo, K.; Li, H.; Yu, Z. Size-Dependent Catalytic Activity of Monodispersed Nickel Nanoparticles for the Hydrolytic Dehydrogenation of Ammonia Borane. *ACS Appl. Mater. Interfaces* **2018**, *10* (1), 517–525.

(6) Umegaki, T.; Yan, J. M.; Zhang, X. B.; Shioyama, H.; Kuriyama, N.; Xu, Q. Hollow Ni-SiO2 Nanosphere-Catalyzed Hydrolytic Dehydrogenation of Ammonia Borane for Chemical Hydrogen Storage. *J. Power Sources* **2009**, *191* (2), 209–216.

(7) Wu, Y.; Wu, X.; Liu, Q.; Huang, C.; Qiu, X. Magnetically Recyclable Ni@h-BN Composites for Efficient Hydrolysis of Ammonia Borane. *Int. J. Hydrogen Energy* **2017**, *42* (25), 16003–16011.

(8) Yang, X. J.; Li, L. L.; Sang, W. L.; Zhao, J. L.; Wang, X. X.; Yu, C.; Zhang, X. H.; Tang, C. C. Boron Nitride Supported Ni Nanoparticles as Catalysts for Hydrogen Generation from Hydrolysis of Ammonia Borane. *J. Alloys Compd.* **2017**, *693*, 642–649.

(9) Sun, Y.; Li, X.; Cai, Z.; Bai, H.; Tang, G.; Hou, Z. Synthesis of 3D N-Doped Graphene/Carbon Nanotube Hybrids with Encapsulated Ni NPs and Their Catalytic Application in the Hydrogenation of Nitroarenes. *Catal. Sci. Technol.* **2018**, *8* (19), 4858–4863.

(10) Yang, F.; Wang, M.; Liu, W.; Yang, B.; Wang, Y.; Luo, J.; Tang, Y.; Hou, L.; Li, Y.; Li, Z.; Zhang, B.; Yang, W.; Li, Y. Atomically Dispersed Ni as the Active Site towards Selective Hydrogenation of Nitroarenes. *Green Chem.* **2019**, *21* (3), 704–711.

(11) Zhang, X.; Zhou, Y.; Li, G.; Zhang, L.; Yin, C.; Yang, Y.; Wang, H.; Feng, F.; Wei, L.; Zhang, Q.; Yang, F.; Lin, L.; Lu, C.; Li, X. A Highly Sulfur Resistant and Stable Heterogeneous Catalyst for Liquid-Phase Hydrogenation. *Appl. Catal. B* **2022**, *315*.

(12) He, W.; Jiang, M. M.; Yu, J. X.; Yan, W.; Zhang, X. Y.; Jiang, R.; Zhao, H. F.; Liu, Y.; Feng, F.; Zhang, Q. F.; Lu, C. S.; Li, X. N. Structure-Controlled Graphene-Encapsulated Nickel Nanoparticle with Tailored Work Function to Steer Chemoselective Hydrogenation of Nitroarenes. *Mater. Today Chem.* **2023**, *29*, 101458.

(13) Xie, Z.; Zhang, T.; Zhao, Z. Ni Nanoparticles Grown on SiO2Supports Using a Carbon Interlayer Sacrificial Strategy for Chemoselective Hydrogenation of Nitrobenzene Andm-Cresol. *ACS Appl. Nano. Mater.* **2021**, *4* (9), 9353–9360.

(14) She, W.; Qi, T.; Cui, M.; Yan, P.-F.; Seik Weng, N.; Li, W.; Li, G.-M.; Qi, T.; Yan, P.; Weng Ng, S.; Li, G. High Catalytic Performance of CeO2-Supported Ni Catalyst for Hydrogenation of Nitroarenes Fabricated via Coordination-Assisted Strategy. *ACS Appl. Mater. Interfaces* **2018**, *10* (17), 14698-14707.

(15) Dong, L.; Liu, Z.; Wang, Y.; Lan, Y.; Chen, C.; Zhang, W. Ni-Based Nanocatalyst Protected by Ultrathin Mesoporous Nitrogen-Doped Carbon Layer with Hollow Structure for the Efficient Transfer Hydrogenation of Halogenated Nitrobenzenes. *Mol. Catal*. **2023**, *547*, 113339.

(16) Feng, B.; Guo, R.; Cai, Q.; Song, Y.; Li, N.; Fu, Y.; Chen, D. L.; Zhang, J.; Zhu, W.; Zhang, F. Construction of Isolated Ni Sites on Nitrogen-Doped Hollow Carbon Spheres with Ni–N3 Configuration for Enhanced Reduction of Nitroarenes. *Nano. Res.* **2022**, *15* (7), 6001–6009.

(17) Romanazzi, G.; Fiore, A. M.; Mali, M.; Rizzuti, A.; Leonelli, C.; Nacci, A.; Mastrorilli, P.; Dell'Anna, M. M. Polymer Supported Nickel Nanoparticles as Recyclable Catalyst for the Reduction of Nitroarenes to Anilines in Aqueous Medium. *Mol. Catal.* **2018**, *446*, 31–38.

(18) Basaveni, S.; Kuchkina, N. V.; Shifrina, Z. B.; Pal, M.; Rajadurai, M. Ni Nanoparticles on Polyaromatic Hyperbranched Polymer Support as a Mild, Tunable, and Sustainable Catalyst for Catalytic Transfer Hydrogenation. *J. Nanopart. Res.* **2019**, *21* (5), 1-14.

(19) Mohapatra, S. K.; Sonavane, S. U.; Jayaram, R. V.; Selvam, P. Regio- and Chemoselective Catalytic Transfer Hydrogenation of Aromatic Nitro and Carbonyl as Well as Reductive Cleavage of Azo Compounds over Novel Mesoporous NiMCM-41 Molecular Sieves. *Org. Lett.* **2002**, *4* (24), 4297–4300.